

Optimal Projections for Classification with Naïve Bayes

David P. Hofmeyr

School of Mathematical Sciences, Lancaster University, United Kingdom

Francois Kamper

Swiss Data Science Center, EPFL, Switzerland

Machail M. Melonas

Kohort, South Africa

Abstract

In the Naïve Bayes classification model the class conditional densities are estimated as the products of their marginal densities along the cardinal basis directions. We study the problem of obtaining an alternative basis for this factorisation with the objective of enhancing the discriminatory power of the associated classification model. We formulate the problem as a projection pursuit to find the optimal linear projection on which to perform classification. Optimality is determined based on the multinomial likelihood within which probabilities are estimated using the Naïve Bayes factorisation of the projected data. Projection pursuit offers the added benefits of dimension reduction and visualisation. We discuss an intuitive connection with class conditional independent components analysis, and show how this is realised visually in practical applications. The performance of the resulting classification models is investigated using a large collection of (162) publicly available benchmark data sets and in comparison with relevant alternatives. We find that the proposed approach substantially outperforms other popular probabilistic discriminant analysis models and is highly competitive with Support Vector Machines.

Keywords: classification; mixture model; dimension reduction; data visualisation; discriminant analysis; Naïve Bayes; kernel density estimation; projection pursuit; Independent Component Analysis

1 Introduction

Suppose we are presented with pairs $(y_1, \mathbf{x}_1), \dots, (y_n, \mathbf{x}_n)$ assumed to have arisen independently from some joint probability distribution, $P_{Y,X}$, on $[K] \times \mathbb{R}^p$, where we have used $[K]$ to denote the first K natural numbers, i.e., $[K] = \{1, \dots, K\}$. That is,

the *class labels*, $\{y_1, \dots, y_n\}$, each take one of K known and distinct values and the associated vectors of *covariates*, $\{\mathbf{x}_1, \dots, \mathbf{x}_n\}$, are each p -dimensional real valued vectors. The problem of discriminant analysis in a probabilistic framework is to obtain an estimate of the *posterior probability* of class membership, $P(Y = k|X = \mathbf{x})$, for each $k \in [K]$, based on a simple application of Bayes' rule,

$$P(Y = k|X = \mathbf{x}) = \frac{\pi_k f_{X|Y=k}(\mathbf{x})}{\sum_{j=1}^K \pi_j f_{X|Y=j}(\mathbf{x})}, \quad (1)$$

where $\pi_k = P(Y = k)$ is the *prior probability* for class k , and we use the general notation “ f_Z ” to represent the probability density function¹ of the random variable Z . Different approaches to the problem vary according to how they estimate the densities $f_{X|Y=k}$, where it is almost universal that the prior probabilities are estimated using $\hat{\pi}_k = \frac{n_k}{n}$, for $n_k = \sum_{i=1}^n \mathbf{1}(y_i = k)$, where $\mathbf{1}(\cdot)$ is the indicator function. Popular approaches include treating each such *class conditional density* as a Gaussian density with appropriately estimated mean vector and covariance matrix (Fisher, 1936; Lachenbruch and Goldstein, 1979), and using non-parametric density estimators (Hand, 1982).

The non-parametric variant of discriminant analysis is appealing for its flexibility. However, this flexibility comes at the cost of increased estimation variance, as well as computational complexity. A popular simplification, referred to as *Naïve Bayes*, addresses some of these limitations of density estimation by treating the densities of the random variables $X|Y = k; k \in [K]$, as admitting a simple factorisation over their margins. That is, $\hat{f}_{X|Y=k} = \prod_{d=1}^p \hat{f}_{X_d|Y=k}$, where X_d is the d -th component of the p -dimensional X , and $\hat{f}_{X_d|Y=k}$ is a univariate density estimator. This *class conditional independence* approach generally introduces bias into the estimated den-

¹For simplicity we discuss the scenario in which X is a continuous random variable, but acknowledge the scope for a more general formulation of the posterior class probabilities in the presence of discrete or mixed covariates. Note also that because our approach is based on the marginal distributions of (non-sparse) linear projections of X , the conditions under which a formulation in terms of continuous X is appropriate are quite general. We provide a brief discussion of this in the following section.

sities, however it has been observed that in many cases the effect which this has on the accurate estimation of the class decision boundaries is fairly minimal. The class decision boundaries are the surfaces of the sets

$$\left\{ \mathbf{x} \in \mathbb{R}^p \left| \operatorname{argmax}_{k \in [K]} P(Y = k | X = \mathbf{x}) = j \right. \right\}; j \in [K]. \quad (2)$$

That is to say, from the point of view of accurate classification, our primary concern is not the most accurate estimation of the probabilities $P(Y = k | X = \mathbf{x}); k \in [K]$, but rather which of these probabilities is dominant, i.e., of $\operatorname{argmax}_{k \in [K]} P(Y = k | X = \mathbf{x})$; and in many instances this estimation problem suffers less from the Naïve Bayes formulation than does the class density estimation problem itself.

In this paper we study the problem of enhancing the classification capabilities of Naïve Bayes. In particular, rather than applying the standard Naïve Bayes factorisation of the class densities over the cardinal basis (i.e., over the coordinate dimensions of \mathbb{R}^p), we seek to find an optimal basis over which to perform this factorisation. In particular, we formulate the problem as a projection pursuit in which the objective is given by the multinomial likelihood, where probabilities in this likelihood are determined according to Eq. (1), with class densities estimated using the Naïve Bayes factorisation on the projected data. This has the potential to extend the collection of problems on which Naïve Bayes accurately estimates the class decision boundaries.

A simple two-dimensional example is shown in Figure 1. The figure shows a scenario with three classes in which the class conditional densities factorise along the cardinal basis rotated by $\pi/8$ radians. The plots show the same sample of size 1000 drawn from the underlying distribution, with points from different classes differentiated according to colour and point character. The plots also show the true class decision boundaries as well as those estimated from the sample using Naïve Bayes (NB); the proposed approach (Optimal Projections for Naïve Bayes, OPNB); the Naïve Bayes factorisation applied to the independent components rotation from each class (Class Conditional Independent Components Analysis, CCICA (Bressan and Vitrià, 2002)); and the Naïve Bayes factorisation applied to the “true” ($\pi/8$ rotated cardinal) basis (NB*). Even this relatively moderate rotation results in poor

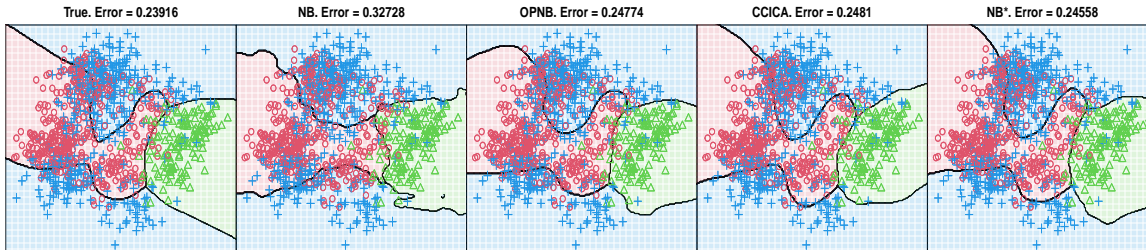


Figure 1: Two-dimensional example in which the class conditional densities factorise over the cardinal basis rotated by $\pi/8$ radians. From left the true class decision boundaries; those estimated using Naïve Bayes (NB) as well as the proposed approach (OPNB); Class Conditional Independent Components Analysis (CCICA); and the Naïve Bayes factorisation applied on the cardinal basis rotated by $\pi/8$ (i.e., the optimal rotation at a population level) are shown. The errors correspond with estimates of the test classification error from samples of size 50000.

performance by the standard Naïve Bayes model, whereas OPNB and CCICA obtain decision boundaries close to those of NB*, and all three have classification error close to the Bayes optimal error rate of 0.23916^2 .

The remaining paper is organised as follows. In Section 2 we provide an explicit description of our problem, and provide technical details of the associated optimisation. We also discuss a connection between this problem and class conditional independent component analysis (Bressan and Vitrià, 2002). In Section 4 we discuss results from experiments with the proposed method. We also document the visualisation capabilities which are offered as a result of finding an optimal projection/basis for the data. We conclude the paper with a discussion in Section 5.

²The classification error of the different models was estimated from a test sample of size 50000, and so may differ very slightly from the population level error rates.

2 Optimal Projections for Discrimination with Naïve Bayes Probabilities

In this section we provide an explicit formulation of the objective we address, and discuss technicalities associated with its optimisation. At its essence, our focus is on obtaining an alternative factorisation of the class conditional densities to that used in Naïve Bayes. We address this problem by formulating it as a projection pursuit, in which we seek a *projection matrix*, $\mathbf{V} \in \mathbb{R}^{p \times p'}$, for which the factorisation of the estimated densities of the random variables $\mathbf{V}^\top X|Y = k$; $k \in [K]$, leads to improved classification accuracy over that arising from the factorisation of the estimated densities of $X|Y = k$; $k \in [K]$, as in the standard Naïve Bayes approach. An added benefit of treating this as a projection pursuit is the possibility for using it to perform dimension reduction, i.e., when $p' < p$. The objective we use to optimise the projection matrix is the multinomial likelihood, given by

$$\mathcal{L}(\mathbf{V}) \propto \prod_{i=1}^n \frac{\hat{\pi}_{y_i} \hat{f}_{\mathbf{V}^\top X|Y=y_i}(\mathbf{V}^\top \mathbf{x}_i)}{\sum_{k=1}^K \hat{\pi}_k \hat{f}_{\mathbf{V}^\top X|Y=k}(\mathbf{V}^\top \mathbf{x}_i)}. \quad (3)$$

Existing projection pursuit methods in the literature which utilise this multinomial likelihood include those based using Gaussian class densities (Hofmeyr et al., 2023) and Gaussian mixtures for the class densities (Peltonen and Kaski, 2005).

2.1 Optimising $\mathcal{L}(\mathbf{V})$

As is common, we optimise the logarithm of the likelihood, which is thus given by (up to an additive constant)

$$\ell(\mathbf{V}) = \sum_{i=1}^n \left(\log \left(\hat{\pi}_{y_i} \hat{f}_{\mathbf{V}^\top X|Y=y_i}(\mathbf{V}^\top \mathbf{x}_i) \right) - \log \left(\sum_{k=1}^K \hat{\pi}_k \hat{f}_{\mathbf{V}^\top X|Y=k}(\mathbf{V}^\top \mathbf{x}_i) \right) \right), \quad (4)$$

where with the Naïve Bayes factorisation each estimated class density is given by

$$\hat{f}_{\mathbf{V}^\top X|Y=y_i}(\mathbf{V}^\top \mathbf{x}) = \prod_{d=1}^{p'} \hat{f}_{\mathbf{V}_d^\top X|Y=y_i}(\mathbf{V}_d^\top \mathbf{x}), \quad (5)$$

where we use \mathbf{V}_d to be the d -th column of \mathbf{V} . The factorisation allows us to use efficient methods for univariate kernel density estimation to evaluate the objective. In particular, we set

$$\hat{f}_{\mathbf{V}_d^\top X|Y=k}(x) = \frac{1}{n_k h_k} \sum_{i:y_i=k} K\left(\frac{x - \mathbf{V}_d^\top \mathbf{x}_i}{h_k}\right), \quad (6)$$

where K is a kernel function. We use the smooth order 1 kernel described in Hofmeyr (2019), and given by $K(x) \propto (|x| + 1) \exp(-|x|)$, as it has been found to be effective for efficient projection pursuit based on kernel densities (Hofmeyr, 2019, 2022).

A common constraint in estimating optimal projections is to control scaling issues by forcing the columns of \mathbf{V} to have unit length. We only implicitly enforce this constraint by addressing the optimisation problem

$$\max_{\mathbf{V} \in \mathbb{R}^{p \times p'}} \ell(\vec{\mathbf{V}}), \text{ where} \quad (7)$$

$$\vec{\mathbf{V}} = \mathbf{V} \text{diag}(\|\mathbf{V}_1\|, \dots, \|\mathbf{V}_{p'}\|)^{-1} \in \mathbb{R}^{p \times p'} \quad (8)$$

has as d -th column $\frac{1}{\|\mathbf{V}_d\|} \mathbf{V}_d$. That is, in order to optimise the projection we perform the normalisation of the columns of \mathbf{V} within evaluation of the objective function. This requires modification of the gradient of the function as well, which we discuss next.

It will be convenient, for the sake of brevity, to introduce the following notation. We will use Z to represent the projection of the random variable, $\mathbf{V}^\top X$, and \mathbf{z}_i or \mathbf{z} to represent the projected data point $\mathbf{V}^\top \mathbf{x}_i$, or an arbitrary realisation, $\mathbf{V}^\top \mathbf{x}$, respectively. To shorten class conditioning notation $\cdot|Y = j$, we will henceforth simply write $\cdot|j$, so that, in total, when there is no ambiguity about the value of \mathbf{V} , we can write $\hat{f}_{Z|j}(\mathbf{z})$ for $\hat{f}_{\mathbf{V}^\top X|Y=j}(\mathbf{V}^\top \mathbf{x})$. In addition, we will use the subscript \bar{t} to mean all-but-the- t -th, so that $Z_{\bar{t}} = (Z_1, \dots, Z_{t-1}, Z_{t+1}, \dots, Z_{p'})$, and similarly $\mathbf{z}_{i\bar{t}} = (z_{i1}, \dots, z_{i(t-1)}, z_{i(t+1)}, \dots, z_{ip'})$. This is particularly useful in the context of factorising densities, e.g., $\hat{f}_{Z|j}(\mathbf{z}) = \hat{f}_{Z_{\bar{t}}|j}(\mathbf{z}_{\bar{t}}) \hat{f}_{Z_t|j}(z_t)$. Finally, we set $\hat{f}_Z = \sum_{j=1}^K \hat{\pi}_j \hat{f}_{Z|j}$.

In order to derive an expression for the gradient of $\ell(\vec{\mathbf{V}})$, we will write

$$\ell(\vec{\mathbf{V}}) = \tilde{\ell}(\mathbf{Z}), \quad (9)$$

$$\tilde{\ell}(\mathbf{Z}) := \sum_{i=1}^n \left(\log \left(\hat{\pi}_{y_i} \hat{f}_{Z|y_i}(\mathbf{z}_i) \right) - \log \left(\sum_{k=1}^K \hat{\pi}_k \hat{f}_{Z|k}(\mathbf{z}_i) \right) \right), \quad (10)$$

$$\mathbf{Z} := \mathbf{X}\vec{\mathbf{V}}, \quad (11)$$

with $\mathbf{X} \in \mathbb{R}^{n \times p}$ the matrix with observations stored row-wise.

Now, since the effect of varying the t -th column of \mathbf{V} only affects the t -th column of \mathbf{Z} , we can then evaluate the vector of partial derivatives of $\ell(\vec{\mathbf{V}})$, with respect to the elements in the t -th column of \mathbf{V} , using the chain rule decomposition

$$\nabla_{\mathbf{V}_t} \ell(\vec{\mathbf{V}}) = \nabla_{\mathbf{Z}_t} \tilde{\ell}(\mathbf{Z}) D_{\mathbf{V}_t} \mathbf{Z}_t, \quad (12)$$

where $D_{\mathbf{V}_t} \mathbf{Z}_t$ is the matrix with i, j -th entry $\frac{\partial z_{it}}{\partial \mathbf{V}_{jt}}$, and so

$$D_{\mathbf{V}_t} \mathbf{Z}_t = \frac{1}{\|\mathbf{V}_t\|} \mathbf{X} \left(\mathbf{I} - \frac{1}{\|\mathbf{V}_t\|^2} \mathbf{V}_t \mathbf{V}_t^\top \right). \quad (13)$$

In order to evaluate the elements of $\nabla_{\mathbf{Z}_t} \tilde{\ell}(\mathbf{Z})$, consider that

$$\begin{aligned} \frac{\partial \tilde{\ell}(\mathbf{Z})}{\partial z_{st}} &= \sum_{i=1}^n \left(\frac{\frac{\partial}{\partial z_{st}} \hat{f}_{Z|y_i}(\mathbf{z}_i)}{\hat{f}_{Z|y_i}(\mathbf{z}_i)} - \frac{\frac{\partial}{\partial z_{st}} \hat{f}_Z(\mathbf{z}_i)}{\hat{f}_Z(\mathbf{z}_i)} \right) \\ &= \sum_{i=1}^n \left(\frac{\frac{\partial}{\partial z_{st}} \prod_{d=1}^{p'} \hat{f}_{Z_d|y_i}(z_{id})}{\prod_{d=1}^{p'} \hat{f}_{Z_d|y_i}(z_{id})} - \frac{\sum_{j=1}^K \hat{\pi}_j \frac{\partial}{\partial z_{st}} \prod_{d=1}^{p'} \hat{f}_{Z_d|j}(z_{id})}{\hat{f}_Z(\mathbf{z}_i)} \right) \\ &= \sum_{i:y_i=y_s} \frac{\frac{\partial}{\partial z_{st}} \hat{f}_{Z_t|y_s}(z_{it})}{\hat{f}_{Z_t|y_s}(z_{it})} - \sum_{i=1}^n \frac{\sum_{j=1}^K \hat{\pi}_j \hat{f}_{Z_{\bar{t}}|j}(\mathbf{z}_{i\bar{t}}) \frac{\partial}{\partial z_{st}} \hat{f}_{Z_t|j}(z_{it})}{\hat{f}_Z(\mathbf{z}_i)}, \end{aligned}$$

where the first sum in the final expression only includes those observations from the same class as \mathbf{x}_s since changes to the value of \mathbf{z}_s will not affect the estimated densities of other projected points evaluated in *their* class densities. To obtain an explicit expression for these partial derivatives, we proceed with the simpler first

term to begin;

$$\begin{aligned}
T_1 &:= \sum_{i:y_i=y_s} \frac{\frac{\partial}{\partial z_{st}} \hat{f}_{Z_t|y_s}(z_{it})}{\hat{f}_{Z_t|y_s}(z_{it})} \\
&= \sum_{\substack{i:y_i=y_s \\ i \neq s}} \frac{\frac{\partial}{\partial z_{st}} \hat{f}_{Z_t|y_s}(z_{it})}{\hat{f}_{Z_t|y_s}(z_{it})} + \frac{\frac{\partial}{\partial z_{st}} \hat{f}_{Z_t|y_s}(z_{st})}{\hat{f}_{Z_t|y_s}(z_{st})} \\
&= \sum_{\substack{i:y_i=y_s \\ i \neq s}} \frac{1}{\hat{f}_{Z_t|y_s}(z_{it})} \frac{1}{n_{y_s} h_{y_s}} \sum_{j:y_j=y_s} \frac{\partial}{\partial z_{st}} K \left(\frac{z_{jt} - z_{it}}{h_{y_s}} \right) + \frac{1}{\hat{f}_{Z_t|y_s}(z_{st})} \frac{1}{n_{y_s} h_{y_s}} \sum_{j:y_j=y_s} \frac{\partial}{\partial z_{st}} K \left(\frac{z_{jt} - z_{st}}{h_{y_s}} \right) \\
&= \frac{1}{n_{y_s} h_{y_s}^2} \sum_{i:y_i=y_s} K' \left(\frac{z_{st} - z_{it}}{h_{y_s}} \right) \left(\frac{1}{\hat{f}_{Z_t|y_s}(z_{it})} + \frac{1}{\hat{f}_{Z_t|y_s}(z_{st})} \right).
\end{aligned}$$

Note that $K' \left(\frac{z_{st} - z_{st}}{h_{y_s}} \right) = 0$, and hence both sums can be taken over all $i : y_i = y_s$. Now, with the explicit form of the terms $\hat{f}_{Z_t|j}(z_{it})$, the negative of the second term in the partial derivative is given by

$$-T_2 := \sum_{i=1}^n \frac{1}{\hat{f}_Z(\mathbf{z}_i)} \sum_{j=1}^K \hat{\pi}_j \hat{f}_{Z_{\bar{i}|j}}(\mathbf{z}_{i\bar{i}}) \frac{1}{n_j h_j} \sum_{l:y_l=j} \frac{\partial}{\partial z_{st}} K \left(\frac{z_{lt} - z_{it}}{h_j} \right),$$

where the non-zero partial derivatives occur only if either index i or l is equal to s . We thus have,

$$\begin{aligned}
-T_2 &= \frac{1}{\hat{f}_Z(\mathbf{z}_s)} \sum_{j=1}^K \frac{\hat{f}_{Z_{\bar{i}|j}}(\mathbf{z}_{s\bar{i}})}{n h_j^2} \sum_{l:y_l=j} K' \left(\frac{z_{st} - z_{lt}}{h_j} \right) + \sum_{i=1}^n \frac{1}{\hat{f}_Z(\mathbf{z}_i)} \frac{\hat{f}_{Z_{\bar{i}|y_s}}(\mathbf{z}_{i\bar{i}})}{n h_{y_s}^2} K' \left(\frac{z_{st} - z_{it}}{h_{y_s}} \right) \\
&= \frac{1}{n} \sum_{i=1}^n \left(\frac{\hat{f}_{Z_{\bar{i}|y_i}}(\mathbf{z}_{s\bar{i}})}{h_{y_i}^2 \hat{f}_Z(\mathbf{z}_s)} K' \left(\frac{z_{st} - z_{it}}{h_{y_i}} \right) + \frac{\hat{f}_{Z_{\bar{i}|y_s}}(\mathbf{z}_{i\bar{i}})}{h_{y_s}^2 \hat{f}_Z(\mathbf{z}_i)} K' \left(\frac{z_{st} - z_{it}}{h_{y_s}} \right) \right).
\end{aligned}$$

These expressions for the terms T_1 and T_2 are now in the form described by Hofmeyr (2019), for which computation for all s is possible in $\mathcal{O}(n \log n)$ time.

2.1.1 Other Practicalities

Discrete covariates: One of the appealing properties of the standard Naïve Bayes model is its ability to easily incorporate both continuous and discrete covariates, whereas in general modelling multivariate discrete covariates or combinations of discrete and

continuous covariates in a probabilistic classification model, i.e., one which explicitly models the class conditional distributions, might be extremely challenging. This is especially important when the discrete covariates are categorical and the ordering of and relative differences between the values with which they are encoded may be arbitrary.

One of the most common approaches for incorporating categorical covariates is one-hot-encoding (OHE), in which a covariate taking G distinct values is replaced with $G-1$ binary (0/1) variables, and is then treated as a numerical variable. Although this alleviates the problem of arbitrary differences and ordering; problems of discreteness remain, especially if some of the resulting binary variables are constant within some classes.

In the projection pursuit framework where the projection matrix, \mathbf{V} , is dense (contains no zeroes), all of the random variables $\mathbf{V}_d^\top X; d = 1, \dots, p'$ are continuous as long as there is even a single covariate whose support is the entire real line. Furthermore, even if there are no such continuous covariates, dense projections of multiple binary variables arising from OHE will often assume a large number of distinct values and so modelling them as continuous often leads to reliable estimation of classification models.

It is worth noting that this benefit does not extend to models which are invariant to rotation of covariates (as are many classification models) since the joint distribution of $\mathbf{V}^\top X$ is not continuous even if each of its marginal distributions is.

Initialisation: The objective function given in Eq. (4) is non-concave and so initialisation of \mathbf{V} can have a strong impact on the quality of the resulting model. We anticipate that in many cases the optimal \mathbf{V} will be one which expresses a strong discrimination of classes through the separation of their means. Based on this we initialise \mathbf{V} heuristically using the discriminant vectors obtained in linear discriminant analysis (LDA). That is, we initialise \mathbf{V} using the leading eigenvectors of the matrix $\hat{\Sigma}_W^{-1} \hat{\Sigma}_B$ where $\hat{\Sigma}_W$ is a pooled estimate of the within class covariance and is

proportional to $\sum_{i=1}^n (\mathbf{x}_i - \hat{\boldsymbol{\mu}}_{y_i})(\mathbf{x}_i - \hat{\boldsymbol{\mu}}_{y_i})'$ where $\hat{\boldsymbol{\mu}}_1, \dots, \hat{\boldsymbol{\mu}}_K$ are the class mean vectors and $\hat{\Sigma}_B$ is the contribution to the total data covariance coming from between the classes and is proportional to $\sum_{i=1}^n (\hat{\boldsymbol{\mu}}_{y_i} - \hat{\boldsymbol{\mu}})(\hat{\boldsymbol{\mu}}_{y_i} - \hat{\boldsymbol{\mu}})'$, with $\hat{\boldsymbol{\mu}}$ the overall data mean vector combining all classes. Note that since there are at most $K - 1$ non-arbitrary eigenvectors of $\hat{\Sigma}_W^{-1}\hat{\Sigma}_B$, whenever we desire a larger projection we initialise the remaining columns of \mathbf{V} using the principal components of the data projected into the null space of these LDA discriminant vectors.

3 Connection to Class Conditional Independent Component Analysis

Independent Component Analysis (Comon, 1994, ICA) is a projection pursuit problem that seeks the projection matrix, \mathbf{V} , which minimises a measure of statistical dependence in the elements of $\mathbf{V}^\top X$, where X is the random variable assumed to underlie ones observations. A popular measure of dependence in ICA is the mutual information. It can be shown that an equivalent problem is to minimise the sum of the differential entropies of the random variables $\mathbf{V}_1^\top X, \dots, \mathbf{V}_{p'}^\top X$, i.e., to minimise

$$\sum_{d=1}^{p'} E \left[-\log \left(f_{\mathbf{V}_d^\top X}(\mathbf{V}_d^\top X) \right) \right]. \quad (14)$$

There is an inherent and intuitive connection between ICA and Naïve Bayes, since the factorisation used in Naïve Bayes treats the random variables $X|Y = k; k \in [K]$, as having independent entries. Indeed, a variation of non-parametric discriminant analysis applies ICA to the subsets of the data arising in each of the classes, before using a Naïve Bayes factorisation in order to estimate the class densities (Bressan and Vitrià, 2002). This is an appealing idea for its simplicity, and the method has shown some success. However, as the projection matrices are obtained separately for each class, there is no reason to expect any of these will be useful for the discrimination of classes. In other words, this method is motivated by obtaining more accurate

estimates of the class densities by combining ICA with Naïve Bayes factorisation, but the estimation procedure is fully agnostic of the actual classification objective.

Let us now turn our attention to the log-likelihood objective we consider, given in Eq. (4). The first term is given by

$$\begin{aligned}
& \sum_{i=1}^n \log \left(\hat{\pi}_{y_i} \hat{f}_{\mathbf{V}^\top X|y_i}(\mathbf{V}^\top \mathbf{x}_i) \right) = \\
& \sum_{k=1}^K \left(n_k \log(\hat{\pi}_k) + \sum_{i:y_i=k} \sum_{d=1}^{p'} \log \left(\hat{f}_{\mathbf{V}_d^\top X|k}(\mathbf{V}_d^\top \mathbf{x}_i) \right) \right) \\
& = C + \sum_{k=1}^K n_k \sum_{d=1}^{p'} \frac{1}{n_k} \sum_{i:y_i=k} \log \left(\hat{f}_{\mathbf{V}_d^\top X|k}(\mathbf{V}_d^\top \mathbf{x}_i) \right) \\
& = C + \sum_{k=1}^K n_k \sum_{d=1}^{p'} \overline{\log \left(\hat{f}_{\mathbf{V}_d^\top X|k}(\mathbf{V}_d^\top \mathbf{x}) \right)},
\end{aligned}$$

where $\overline{\log \left(\hat{f}_{\mathbf{V}_d^\top X|k}(\mathbf{V}_d^\top \mathbf{x}) \right)}$ is supposed to represent the empirical average of the estimated log density for class k , and C is a constant independent of \mathbf{V} . By replacing the expectations in the ICA objective, Eq. (14), with their empirical estimates, we can see that the first term in our objective is simply the weighted sum of the ICA objectives for the subsets of the data belonging to each class (recall that our objective is to maximise the log-likelihood, whereas ICA minimises the differential entropy, or equivalently maximises the negative entropy). This is appealing since this part of the objective encourages our solution to have low dependence in the elements of the random variables $\mathbf{V}^\top X|Y = k; k \in [K]$, and hence the Naïve Bayes factorisation is likely to lead to relatively accurate estimation of the class densities. While this is a desirable property, as previously discussed, the discrimination of classes does not yet factor in. The negative of the second term in our objective is given by

$$\sum_{i=1}^n \log \left(\sum_{k=1}^K \hat{\pi}_k \hat{f}_{\mathbf{V}^\top X|k}(\mathbf{V}^\top \mathbf{x}_i) \right).$$

This term measures the estimated total (mixture) log-likelihood of the projected points. This can be thought of as a penalty which discourages projection matrices,

\mathbf{V} , upon which the projected points are fit well by the density which incorporates all of the classes. In other words the first term encourages a good fit of the points in their own classes, while the second term ensures points aren't simply well explained by all of the classes as this would not allow strong discrimination.

4 Experiments

In this section we explore the classification accuracy of the proposed approach in comparison with relevant alternatives, on a large collection of publicly available benchmark data sets. We also perform an investigation into the relationships between the classification performance of the proposed approach and the characteristics of the data to which it is applied.

4.1 Data Sets and Preprocessing

For our experiments, we considered all 162 classification data sets given in Olson et al. (2017). We conducted the following preprocessing policy, which was executed in order:

1. For data sets containing more than 3000 samples we performed stratified sampling to obtain a sample of size 3000 which (approximately) respects the class proportions in the complete data set.
2. We removed classes with fewer than 10 observations from the data.
3. Covariates with zero sample standard deviation were excluded from the experiments.
4. Covariates with at most 5 unique values were treated as categorical and one-hot encoded.
5. Small Gaussian perturbations were added to the data to avoid numerical issues, arising when variables have zero standard deviation within one of the classes.

The standard deviation of the perturbations added to a covariate was equal to one percent of the standard deviation of the covariate itself.

6. If a data set contains more than 300 covariates then we replace them with their first 300 principal components.

4.2 Classification models, Tuning, and Evaluation

Our focus is mainly on alternative probabilistic classification models, i.e., those using applications of Bayes' Rule applied to posterior probabilities of class membership arising from estimated class conditional distributions. But for context we also included the popular Support Vector Machine (Cortes and Vapnik, 1995, SVM). Below is a complete list of the models we considered, along with their respective tuning parameters.

1. Naïve Bayes (NB): The Naïve Bayes model with class conditional marginal densities estimated using KDE. Note that using standard bandwidth selection rules for KDE is not appropriate for discrete covariates. When tuning bandwidths we therefore separate the OHE encoded categorical covariates from the continuous ones and tune a single bandwidth $\alpha \in \{0.1, 0.2, \dots, 0.5\}$ to be used for all classes and all binary variables, and a single multiplication factor, $\gamma \in \{1/3, 1/2, 1, 2, 3\}$, and set the bandwidth for a pair of class and continuous covariate equal to γ multiplied by Silverman's rule of thumb value (Silverman, 2018) for the corresponding subset of points. Note that using an over-smoothing bandwidth on OHE encoded categorical variables is very similar in the resulting probabilities to applying a Laplace adjustment to the empirical proportions in the different values of the categorical variable(s).

Note that we also considered the Gaussian Naïve Bayes model, in which the class conditional marginals are treated as Gaussian, but the performance of this approach was overall worse than all other methods to the extent that its

inclusion made the comparison between other methods more challenging, and so we omit these results.

2. Class Conditional ICA + Naïve Bayes (CCICA): The method of Bressan and Vitrià (2002) in which class conditional densities are estimated from the product of the marginal density estimates of the ICA transformed classes. We tuned both the (shared) dimension of the ICA transformations for the classes, from the set $[\min\{p, 20\}]$; and also a bandwidth multiplier for the KDE estimates of the marginal densities, using the same approach as for NB. Note that the issues of handling one-hot-encoded variables using non-parametric density estimates is mitigated in the same way by CCICA as in the proposed approach and so it is not necessary to modify these density estimates for discrete covariates (nor is it clear how this could be appropriately done).
3. Kernel Density Discriminant Analysis (KDDA): The probabilistic classification model in which class densities are estimated with a multivariate kernel estimator. To accommodate the continuous as well as one-hot-encoded variables we used diagonal bandwidth matrices for each class, and tuned hyperparameters α and γ from the same sets as for Naïve Bayes. The bandwidth matrix for class k was then, assuming w.o.l.o.g. that the continuous covariates lie in the leading columns of the data matrix, set to

$$\begin{bmatrix} \gamma \left(\frac{4}{n_k(p_c+2)} \right)^{\frac{1}{p_c+4}} \Delta(\hat{\Sigma}_k)^{1/2} & \mathbf{0} \\ \mathbf{0} & \alpha \mathbf{I} \end{bmatrix},$$

where $\Delta(\hat{\Sigma}_k)$ is $\hat{\Sigma}_k$, the sample covariance matrix from class k , but with all off diagonal elements set to zero. Note that the factor $\left(\frac{4}{n_k(p_c+2)} \right)^{\frac{1}{p_c+4}}$, where p_c is the number of continuous covariates, arises from Silverman’s rule of thumb when using a Gaussian kernel as we do for KDDA.

4. Linear Discriminant Analysis (LDA): The probabilistic classification model in which class conditional densities are treated as Gaussian, and the maximum

likelihood estimate for a shared covariance matrix is used. We tuned the number of discriminant dimensions to use for classification (number of eigenvectors of the matrix $\hat{\Sigma}_W^{-1}\hat{\Sigma}_B$, which we described in relation to our initialisation of \mathbf{V}).

5. Regularised Discriminant Analysis (RDA): The probabilistic classification model with Gaussian class densities in which class k is given covariance matrix $\lambda\hat{\Sigma}_k + (1 - \lambda)\hat{\Sigma}_W$, where $\hat{\Sigma}_k$ is the maximum likelihood estimate of the covariance of class k and $\hat{\Sigma}_W$ is the shared covariance matrix used in LDA. Tuning over $\lambda \in [0, 1]$ traverses the spectrum of complexity joining LDA for $\lambda = 0$ to Quadratic Discriminant Analysis (QDA) for $\lambda = 1$. We considered values for λ in $\{0.1, 0.2, \dots, 1\}$.
6. Optimal Projections for Gaussian Discriminants (OPGD): A recent method based on classification under a Gaussian discriminant model fit to an optimal projection of the data, as determined by the same multinomial likelihood objective we employ. We tuned only the dimension of the projection, from the set $[\min\{p, 20\}]$.
7. Support Vector Machine (SVM): The kernelised linear classifier based on the penalised hinge-loss objective. We used a Gaussian kernel parameterised as $K(\mathbf{x}_1, \mathbf{x}_2) = \exp(-\alpha\|\mathbf{x}_1 - \mathbf{x}_2\|^2)$, and tuned α over $\{2^{2i+1} | i = -8, -7, \dots, 1\}$ and the “cost” parameter, which balances the trade-off between the ridge-like penalty term and the hinge-loss objective, from the set $\{2^{2i+1} | i = -3, -2, \dots, 7\}$. This collection of values is recommended internally by libsvm (Chang and Lin, 2011) and we used this implementation in our experiments. In libsvm, multi-class classifiers are constructed from binary SVM classifiers in a “one-versus-one” manner.
8. Optimal Projections for Naïve Bayes (OPNB): The proposed method. We set the bandwidth for the k -th class equal to $0.54\gamma(p^{-1}\text{trace}(\hat{\Sigma}_k))^{1/2}n_k^{-0.2}$, where $\gamma \in \{1/3, 1/2, 1, 2, 3\}$ is a single tuning parameter for all classes, as before, and $\hat{\Sigma}_k$ is the sample covariance matrix of the k -th class. This means that

$(p^{-1}\text{trace}(\hat{\Sigma}_k))$ is the average of the variable-wise variances of the k -th class. Note that this setting is inspired by the scaling we used in other non-parametric density estimators (i.e., proportional to Silverman’s rule of thumb³) but because the bandwidth is set before optimising the projection we simplify this to a single average bandwidth per class, rather than setting the bandwidth separately for each class and each projected dimension. For the dimension of the projection we tuned over $p' \in [\min\{p, 20\}]$.

In order to select appropriate tuning parameters we estimated the misclassification rate for each combination using 5-fold cross-validation applied on a training set comprising 75% of a given data set. We then recorded the misclassification rate on the remaining 25% test data, from the model(s) trained on the complete training set with their selected hyperparameters. To mitigate the effects of randomness, we repeated each split into training/test sets 10 times and used the same cross-validation folds for all methods. We also performed stratified sampling at every stage to approximately preserve the class proportions in every test set and cross-validation fold. Because some of the methods applied (including our own) are not scale invariant, for every training instance we scaled the data, dividing each variable by the standard deviation of the corresponding observations within the training set.

4.3 Classification Performance

In this subsection we present summaries of the overall performance of all 8 methods across the 162 data sets. Note that when combining results across data sets of varying characteristics it is important to standardise the performance metric(s) to make them comparable across different data sets. This is because the accuracy achievable across different data sets may differ to the extent that it overshadows the differences in performance between different methods compared on the same data set.

³readers familiar with kernel density estimation with Gaussian kernels will note the factor $0.54 \neq 1.06$, which is because we use the fast kernel smoothing with kernel $K(x) \propto (1 + |x|) \exp(-|x|)$ for which 0.54 is the corresponding constant.

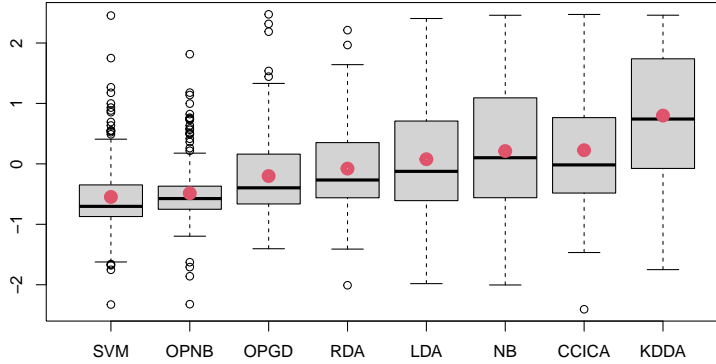


Figure 2: Boxplots of standardised error distributions for all methods across the 162 data sets. The red dots correspond with the averages in each case.

We apply a simple studentisation to standardise the performances of all methods on each of the data sets, so that the standardised error of method M is equal to

$$\frac{Err(M) - \overline{Err}}{S(Err)},$$

where $Err(M)$ is the proportion of (test) misclassifications made by method M on a given data set, and \overline{Err} and $S(Err)$ are the average and standard deviation of the test misclassification proportions from all methods on the data set. Because we performed 10 random training/test splits of each data set, the misclassification proportions of each method were first averaged over these 10 splits before standardisation was applied.

4.3.1 Error Distributions

Boxplots of the distributions of standardised errors achieved by the different methods across all 162 data sets are shown in Figure 2. In addition the averages are shown with red dots. The methods have been ordered based on average standardised error. SVM achieves the lowest standardised error overall, closely followed by OPNB.

Thereafter the three Gaussian discriminant models, OPGD; RDA and LDA achieve similar accuracy to one another, as do NB and CCICA. The performance of KDDA is notably inferior to the other methods.

Recall that SVM is the only non-probabilistic classification method considered, and it is encouraging that the proposed approach is competitive with SVM overall, while substantially outperforming the other probabilistic models.

	OPGD	SVM	LDA	RDA	NB	KDDA	CCICA
OPNB	107-3-52	61-10-91	108-4-50	108-4-50	119-3-40	137-1-24	125-3-34
OPGD		45-5-112	87-6-69	85-4-73	95-1-66	127-0-35	105-4-53
SVM			107-3-52	109-5-48	119-0-43	146-0-16	126-4-32
LDA				72-8-82	94-3-65	110-2-50	82-2-78
RDA					103-1-58	114-2-46	87-3-72
NB						102-2-58	80-2-80
KDDA							57-1-104

Table 1: Comparative performance of pairs of methods. Each cell in the table contains the number of “wins”-“ties”-“losses” by the method listed by row in comparison with the method listed by column. For example OPNB achieves lower error (wins) than OPGD on 107 data sets and higher error (losses) on 52 data sets, while they achieve the same error (ties) on 3 data sets.

It is worth noting that other standardisations of the classification performance are possible, with one alternative being the *percentage-over-best* (Hastie et al., 2009), which simply shifts and scales the errors of all methods on a given data set to span the interval $[0, 1]$. Based on this standardisation the order of the average standardised performance across all data sets remains the same. On the other hand, if no standardisation is applied and the raw misclassification proportions are used then the proposed approach achieves the lowest error and CCICA has a lower error than NB, with all other ranks remaining the same as in the case of standardised errors.

4.3.2 Pair-wise Performance

Although the boxplots allow us to determine relative performances of different methods in general, they do not directly imply any relative comparisons on any individual data sets. Table 1 summarises the pairwise comparative performances for all methods. Each cell in the table shows the number of times the method listed row-wise outperforms (wins); achieves equal performance to (ties); and achieves lower error than (loses) the method listed column-wise. Ignoring instances of equal error (ties), the proposed approach outperforms SVM approximately 40% of the time, and outperforms each other method in at least 60% of cases.

4.4 Dissecting Classification Performance

Here we perform a brief investigation into the relationships between the characteristics of the different data sets and the performance of the different classification methods. Figure 3 shows two heatmaps in which the colour intensity indicates the degree of correlation between the standardised classification error of each classification method and the following data set characteristics:

1. Ratio of categorical variables (cat_rat): The proportion of binary variables in a data set after one-hot-encoding. The reason for taking the number of binary variables rather than the number categorical variables in the original data set is that this accounts for the granularity (number of distinct values) of the categorical variables as well as their number.
2. Class imbalance (imbal): The variance of the class proportions.
3. Number of dimensions (dim): The total number of dimensions after one-hot-encoding.
4. Number of observations (nobs): Recall that we subsampled large data sets down to a maximum of 3000 due to the large computation time required to tune and train all methods on such a large number of data sets.

5. Number of classes (nclass): The total number of classes.
6. Complexity (compl): This is an artificial score designed to capture the degree of complexity of the class distribution(s). It is defined as the ratio of the leave-one-out cross-validation error rate of a 1-nearest-neighbour (1-NN) classifier to that of a nearest-centroid (NC) classifier, which classifies a point solely based on which class mean is the nearest in Euclidean distance⁴. While the 1-NN classifier can accommodate highly non-linear decision boundaries (at the cost of high variance), the NC classifier is very stable (has low variance) but has rigid linear decision boundaries. Although neither is likely to perform well in general, they arguably occupy two ends of the spectrum of complexity and their relative performance can be used to capture to some extent the complexity of the class decision boundaries. Importantly they are also separate from the set of classifiers used for comparison.

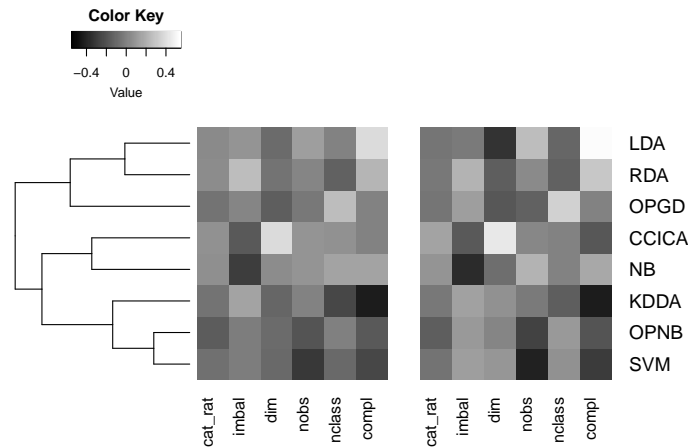


Figure 3: Correlations between standardised error of each method with characteristics of data sets. Left: Marginal correlations, Right: Conditional correlations.

In Figure 3 the left heatmap describes the marginal (linear) relationships between the standardised performance(s) and the data characteristics through their

⁴Variables were standardised before applying the two models

correlations, whereas the right heatmap is supposed to capture the conditional relationships by using the ordinary linear regression coefficients when all variables have been standardised to have unit variance. Note that the performance of the classification methods is based on their standardised error rate, and so darker values in the heatmap(s) suggest that the corresponding method tends to perform well on data showing high values of the corresponding characteristic *relative to the other methods under comparison*. For example, we would expect that all methods will tend to perform relatively better on larger samples than on smaller ones, all other things being equal, which would correspond with dark values in the right heatmap in the “nobs” column. However, by modelling the relative performance of methods in comparison with each other the heatmap arguably represents how much better/worse different methods are at using larger samples; with the simpler LDA and NB models leveraging larger samples the least (light colours in the “nobs” column in the right heatmap) and SVM and OPNB better leveraging larger samples to improve performance. On the other hand the simpler models (as well as the other Gaussian models RDA and OPGD) accommodate additional dimensions far better than the more complex SVM and OPNB.

In addition the figure shows a dendrogram in the left margin based on a complete linkage hierarchical clustering model of the classification models in terms of their relationships with the data characteristics. Some notable take-aways from the figure, for the context of the present study, are that:

- (i) The clustering implied by the dendrogram, although not rigorously designed for purpose, groups OPNB with SVM and KDDA. Moreover, one of the most striking distinguishing data characteristics for these three is their alignment with class complexity (“compl”). While it is intuitively the case that KDDA accommodates highly non-linear decision boundaries⁵ and a well tuned Gaussian

⁵in fact we can see in the heatmaps that KDDA correlates “best” with complexity and LDA “worst”, which should be expected due to their similarities with nearest neighbour and nearest centroid classification, respectively.

SVM will do so too; this suggests the projection pursuit in OPNB is able to turn the relatively inflexible NB into an adaptive and flexible classifier.

It is also worth noting that the validity of this clustering can be reasonably justified by the fact that it groups the three Gaussian discriminant models together, as well as grouping NB with CCICA.

- (ii) Some of the most notable (other) relationships for OPNB are:
 - (a) The strongest negative correlation with “cat_rat” is with OPNB, corroborating our discussion from before in how the dense projections coupled with marginally estimated densities can be an effective way to integrate continuous and categorical variables.
 - (b) Especially after accounting for the effects of the other data characteristics (right heatmap), OPNB tends to perform relatively better as sample size increases (strong negative correlation with nobs), but may perform less well with added classes and highly imbalanced class sizes (positive correlations with nclass and imbal).

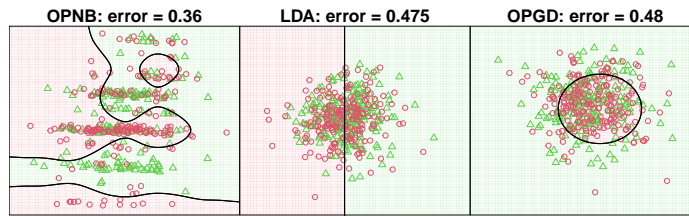
4.5 Projection Plots

As mentioned previously one of the advantages of methods based on projection pursuit (or indeed any form of dimensionality reduction) is that they facilitate interpretation through plots of the projected data. Figure 4 shows three examples taken from the collection of data sets used for accuracy comparisons. These have been selected to show some of the capabilities of the proposed approach, as well as some instances where the performance is relatively poorer. In each of the figures we show the test data (we selected arbitrarily the first of the ten train/test splits for each data set) projected onto a two-dimensional optimised projection obtained using OPNB; LDA; and OPGD, along with the decision boundaries obtained from the training sets. The points in different classes have been differentiated by colour and point character. Since these are only two-dimensional projections (as these offer the most straightforward

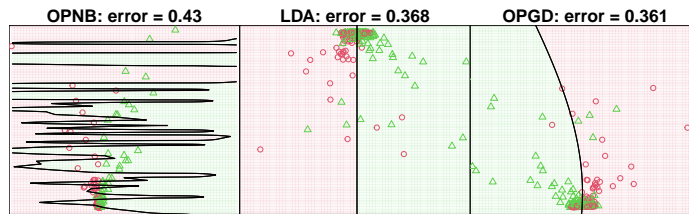
visualisation) the classification performance is generally worse than what is obtained in the experiments reported previously.

Figure 4(a) shows an artificial data set obtained using the GAMETES software, which simulates complex biallelic single nucleotide polymorphism (SNP) disease models designed to be representative of “real” data observed in this context (Urbanowicz et al., 2012). The pmlb repository includes six such data sets, with the example shown in the figure being the third. This example shows the ability of OPNB to separate classes which have multimodal distributions but whose statistics are very similar up to second order, and so are not distinguishable using Gaussian discriminant models. In fact OPNB achieved the best performance from all classification models considered on five of the six GAMETES data sets in the repository, and in the case of the other none of the methods achieved substantially below a randomised classifier, with RDA having the lowest error of 0.472 and CCICA the highest with 0.515.

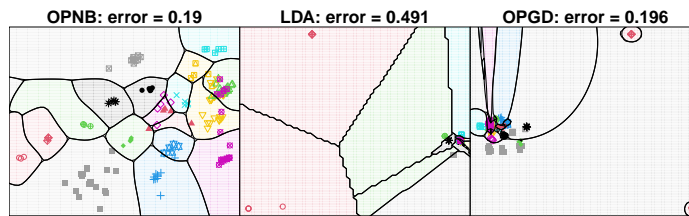
Figure 4(b) shows a simulated data set in which the variables are sequential and each instance either shows a peak/hill or a trough/valley, depending on its class (Graham and Oppacher, 2008). This example was chosen to illustrate a limitation with the current implementation of OPNB; specifically that individual class distributions with scale that varies drastically in different directions may make the assignment of a single bandwidth per class (applied across all projection directions) inappropriate. Nonetheless, it is fortunate that the visualisation of the decision boundaries, as shown in the figure, give a clear diagnosis of the problem. Now, although it is possible to allow the bandwidth to change as the projection is updated during optimisation, this substantially increases the complexity of the gradient computations. Instead we here experimented with a simple pre-scaling alternative, in which the data are first scaled by the inverse square root of the weighted average within class covariance. That is, if $\hat{\Sigma}_W$ is as introduced in relation to the initialisation of \mathbf{V} , then we begin by first multiplying the observations by $\hat{\Sigma}_W^{-1/2}$. Even this simple modification reduced the test error to 0.334. The resulting projection plot can be seen in Figure 5.



(a) Gametes (3)



(b) Hill Valley With Noise



(c) Soybean

Figure 4: Optimal two-dimensional projections from OPNB, LDA and OPGD on three of the data sets used for comparison

Finally, Figure 4(c) shows the Soybean data (Michalski and Chilausky, 1980), which was chosen due to the fact that OPNB achieves very similar accuracy to OPGD, but provides a far more pleasing visualisation; spreading the individual classes more evenly and in such a way that their relative positions and separations are more clearly visible.

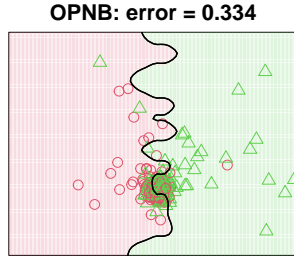


Figure 5: Optimal two-dimensional projection from OPNB on Hill Valley data set after alternative scaling approach.

5 Discussion

The Naïve Bayes model has substantially reduced complexity when compared with other non-parametric discriminant models. However, inevitably the associated reduction in variance comes at the expense of, sometimes substantial, model bias. Unfortunately, although the bias/variance trade-off can be traversed by modifying the bandwidth parameter(s), the rigid model formulation means this traversal is highly limited. In this paper we introduced an intuitive way in which the flexibility of the Naïve Bayes model can be increased within an optimisation based framework, allowing better use of the model’s effective degrees of freedom. By selecting an optimal basis for the factorisation of class conditional densities, this approach has been shown to achieve strong performance across a large collection of benchmark data sets. An investigation into the performance of the method, with reference to the characteristics of the data sets considered, suggests that our approach captures these characteristics more similarly to highly flexible models like SVM and KDDA, than to the inflexible standard Naïve Bayes model. Moreover, the visualisations offered by the model, due to its reliance on projection pursuit, helps to diagnose limitations in the model as well as aid interpretation of the model’s decision boundaries.

References

- Marco Bressan and Jordi Vitrià. Improving naive bayes using class-conditional ica. In *Ibero-American Conference on Artificial Intelligence*, pages 1–10. Springer, 2002.
- Chih-Chung Chang and Chih-Jen Lin. Libsvm: a library for support vector machines. *ACM transactions on intelligent systems and technology (TIST)*, 2(3):1–27, 2011.
- Pierre Comon. Independent component analysis, a new concept? *Signal processing*, 36(3):287–314, 1994.
- Corinna Cortes and Vladimir Vapnik. Support vector machine. *Machine learning*, 20(3):273–297, 1995.
- Ronald A Fisher. The use of multiple measurements in taxonomic problems. *Annals of eugenics*, 7(2):179–188, 1936.
- Lee Graham and Franz Oppacher. Hill-Valley. UCI Machine Learning Repository, 2008. DOI: <https://doi.org/10.24432/C5JC8P>.
- David J Hand. Kernel discriminant analysis. *JOHN WILEY & SONS, INC., ONE WILEY DR., SOMERSET, N. J. 08873, 1982, 264*, 1982.
- Trevor Hastie, Robert Tibshirani, and Jerome Friedman. *The elements of statistical learning: data mining, inference, and prediction*. Springer Science & Business Media, 2009.
- David Hofmeyr. Fast exact evaluation of univariate kernel sums. *IEEE transactions on pattern analysis and machine intelligence*, 2019.
- David P. Hofmeyr. Fast kernel smoothing in r with applications to projection pursuit. *Journal of Statistical Software*, 101(3):1–33, 2022. doi: 10.18637/jss.v101.i03.
- David P Hofmeyr, Francois Kamper, and Michail C Melonas. Optimal projections for gaussian discriminants. *Advances in Data Analysis and Classification*, 17(1):43–73, 2023.

- Peter A Lachenbruch and M Goldstein. Discriminant analysis. *Biometrics*, pages 69–85, 1979.
- R.S. Michalski and R.L. Chilausky. Soybean (Large). UCI Machine Learning Repository, 1980. DOI: <https://doi.org/10.24432/C5JG6Z>.
- Randal S. Olson, William La Cava, Patryk Orzechowski, Ryan J. Urbanowicz, and Jason H. Moore. Pmlb: a large benchmark suite for machine learning evaluation and comparison. *BioData Mining*, 10(1):36, Dec 2017. ISSN 1756-0381. doi: 10.1186/s13040-017-0154-4. URL <https://doi.org/10.1186/s13040-017-0154-4>.
- Jaakko Peltonen and Samuel Kaski. Discriminative components of data. *IEEE Transactions on Neural Networks*, 16(1):68–83, 2005.
- Bernard W Silverman. *Density estimation for statistics and data analysis*. Routledge, 2018.
- Ryan J Urbanowicz, Jeff Kiralis, Nicholas A Sinnott-Armstrong, Tamra Heberling, Jonathan M Fisher, and Jason H Moore. Gametes: a fast, direct algorithm for generating pure, strict, epistatic models with random architectures. *BioData mining*, 5:1–14, 2012.